

Isospin effects in the disappearance of flow as a function of colliding geometry

Sakshi Gautam¹, Aman D. Sood^{2,*} and Rajeev K. Puri¹

¹*Department of Physics, Panjab University, Chandigarh -160 014, India. and*

²*SUBATECH, Laboratoire de Physique Subatomique et des Technologies Associées,
Université de Nantes - IN2P3/CNRS - EMN*

4 rue Alfred Kastler, F-44072 Nantes, France.

(Dated: August 26, 2019)

We study the effect of isospin degree of freedom on the balance energy (E_{bal}) as well as its mass dependence throughout the mass range 48-270 for two sets of isobaric systems with $N/Z = 1$ and 1.4 at different colliding geometries ranging from central to peripheral ones. Our findings reveal the dominance of Coulomb repulsion in isospin effects on E_{bal} as well as its mass dependence throughout the range of the colliding geometry. Our results also indicate that the effect of symmetry energy on E_{bal} is uniform throughout the mass range and throughout the colliding geometry.

PACS numbers: 25.70.Pq, 25.70.-z

I. INTRODUCTION

With the availability of radioactive ion beam (RIB) facilities at Cooler Storage Ring (CSR) (China) [1], the GSI Facility for Antiproton and Ion beam Research (FAIR) [2], RIB facility at Rikagaku Kenyusho (RIKEN) in Japan [3], GANIL in France [4], and the upcoming facility for RIB at Michigan State University [5] one has a possibility to study the properties of nuclear matter under the extreme conditions of isospin asymmetry. Heavy-ion collisions induced by the neutron rich matter provide a unique opportunity to explore the isospin dependence of in-medium nuclear interactions, since isospin degree of freedom plays an important role in heavy-ion collisions through both the nuclear matter equation of state (EOS) as well as via in-medium nucleon-nucleon (nn) cross section.

After about three decades of intensive efforts in both nuclear experiments and theoretical calculations, equation of state for isospin symmetric matter is now relatively well understood. The effect of isospin degree of freedom on the collective transverse in-plane flow as well as on its disappearance [6–8] (there exists a particular incident energy called *balance energy* (E_{bal}) or *energy of vanishing flow* (EVF) at which transverse in-plane flow disappears) has been reported in the literature [9–11], where it was found that neutron-rich systems have higher E_{bal} compared to neutron-deficient systems at all colliding geometries varying from central to peripheral ones. The effect of isospin degree of freedom on E_{bal} was found to be much more pronounced at peripheral colliding geometries compared to central ones. As reported in the literature, the isospin dependence of collective flow as well as its disappearance has been explained as a competition among various reaction mechanisms, such as nucleon-nucleon collisions, symmetry energy, surface property of the colliding nuclei, and Coulomb force. The relative im-

portance among these mechanisms is not yet clear [9]. In recent study, we [12] confronted theoretical calculations (using isospin-dependent quantum molecular dynamics (IQMD) model [13]) with the data at all colliding geometries and were able to reproduce the data within 5% on the average at all colliding geometries. Motivated by the good agreement of the calculations with data, two of us [14] studied the isospin effects on the E_{bal} throughout the mass range 48-350 for two sets of isobaric systems with $N/Z = 1.0$ and 1.4 at semi central colliding geometry. These results showed that the difference between the E_{bal} for two isobaric systems is mainly due to the Coulomb repulsion. It was also shown that Coulomb repulsion dominates over symmetry energy. These findings also indicated towards the dominance of the Coulomb repulsion in larger magnitude of isospin effects in E_{bal} at peripheral collisions. Here we aim to extend the study over full range of colliding geometry varying from central to peripheral ones. Section 2 describes the model in brief. Section 3 explains the results and discussion and Sec. 4 summarizes the results.

II. THE MODEL

The present study is carried out within the framework of IQMD model [13]. The IQMD model treats different charge states of nucleons, deltas, and pions explicitly, as inherited from the Vlasov-Uehling-Uhlenbeck (VUU) model. The IQMD model has been used successfully for the analysis of a large number of observables from low to relativistic energies. The isospin degree of freedom enters into the calculations via symmetry potential, cross sections, and Coulomb interaction.

In this model, baryons are represented by Gaussian-shaped density distributions

$$f_i(\vec{r}, \vec{p}, t) = \frac{1}{\pi^2 \hbar^2} \exp(-[\vec{r} - \vec{r}_i(t)]^2 \frac{1}{2L}) \times \exp(-[\vec{p} - \vec{p}_i(t)]^2 \frac{2L}{\hbar^2}) \quad (1)$$

*Electronic address: amandsood@gmail.com

Nucleons are initialized in a sphere with radius $R = 1.12 A^{1/3}$ fm, in accordance with liquid-drop model. Each nucleon occupies a volume of h^3 , so that phase space is uniformly filled. The initial momenta are randomly chosen between 0 and Fermi momentum (\vec{p}_F). The nucleons of the target and projectile interact by two- and three-body Skyrme forces, Yukawa potential, Coulomb interactions, and momentum-dependent interactions. In addition to the use of explicit charge states of all baryons and mesons, a symmetry potential between protons and neutrons corresponding to the Bethe-Weizsacker mass formula has been included. The hadrons propagate using Hamilton equations of motion:

$$\frac{d\vec{r}_i}{dt} = \frac{d\langle H \rangle}{d\vec{p}_i}; \quad \frac{d\vec{p}_i}{dt} = -\frac{d\langle H \rangle}{d\vec{r}_i} \quad (2)$$

with

$$\begin{aligned} \langle H \rangle &= \langle T \rangle + \langle V \rangle \\ &= \sum_i \frac{p_i^2}{2m_i} + \sum_i \sum_{j>i} \int f_i(\vec{r}, \vec{p}, t) V^{ij}(\vec{r}', \vec{r}) \\ &\quad \times f_j(\vec{r}', \vec{p}', t) d\vec{r}' d\vec{p}' d\vec{p} d\vec{p}'. \end{aligned} \quad (3)$$

The baryon potential V^{ij} , in the above relation, reads as

$$\begin{aligned} V^{ij}(\vec{r}' - \vec{r}) &= V_{Sky}^{ij} + V_{Yuk}^{ij} + V_{Coul}^{ij} + V_{mdi}^{ij} + V_{sym}^{ij} \\ &= [t_1 \delta(\vec{r}' - \vec{r}) + t_2 \delta(\vec{r}' - \vec{r}) \rho^{\gamma-1} (\frac{\vec{r}' + \vec{r}}{2})] \\ &\quad + t_3 \frac{\exp(|(\vec{r}' - \vec{r})|/\mu)}{(|(\vec{r}' - \vec{r})|/\mu)} + \frac{Z_i Z_j e^2}{(|(\vec{r}' - \vec{r})|)} \\ &\quad + t_4 \ln^2[t_5(\vec{p}' - \vec{p})^2 + 1] \delta(\vec{r}' - \vec{r}) \\ &\quad + t_6 \frac{1}{\rho_0} T_{3i} T_{3j} \delta(\vec{r}_i' - \vec{r}_j'). \end{aligned} \quad (4)$$

Here Z_i and Z_j denote the charges of i th and j th baryon, and T_{3i} and T_{3j} are their respective T_3 components (i.e., 1/2 for protons and -1/2 for neutrons). The parameters μ and t_1, \dots, t_6 are adjusted to the real part of the nucleonic optical potential. For the density dependence of the nucleon optical potential, standard Skyrme type parametrization is employed. The momentum-dependence V_{mdi}^{ij} of the nn interactions, which may optionally be used in IQMD, is fitted to the experimental data in the real part of the nucleon optical potential.

III. RESULTS AND DISCUSSION

For the present study, we simulate several thousands events of each reaction at incident energies around E_{bal} in small steps of 10 MeV/nucleon. In particular, we simulate the reactions $^{24}\text{Mg}+^{24}\text{Mg}$, $^{58}\text{Cu}+^{58}\text{Cu}$, $^{72}\text{Kr}+^{72}\text{Kr}$, $^{96}\text{Cd}+^{96}\text{Cd}$, $^{120}\text{Nd}+^{120}\text{Nd}$, $^{135}\text{Ho}+^{135}\text{Ho}$, having $N/Z = 1.0$ and reactions $^{24}\text{Ne}+^{24}\text{Ne}$, $^{58}\text{Cr}+^{58}\text{Cr}$, $^{72}\text{Zn}+^{72}\text{Zn}$, $^{96}\text{Zr}+^{96}\text{Zr}$, $^{120}\text{Sn}+^{120}\text{Sn}$, and $^{135}\text{Ba}+^{135}\text{Ba}$, having $N/Z = 1.4$, respectively, in the whole range of colliding geometry. The colliding geometry is divided into four impact

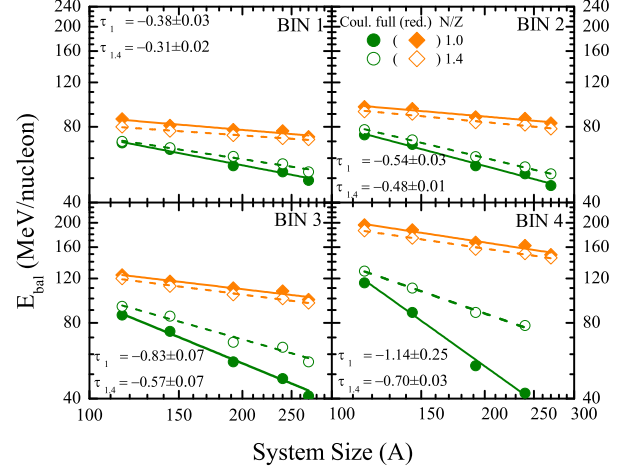


FIG. 1: E_{bal} as a function of combined mass of system for different impact parameter bins. Solid (open) symbols are for systems having $N/Z = 1.0$ (1.4). The solid (dashed) lines are power law fit $\propto A^\tau$. τ values for full Coulomb calculations are displayed in figure. The values of τ for reduced Coulomb calculations are given in the text.

parameter bins of $0.15 < \hat{b} < 0.25$ (BIN 1), $0.35 < \hat{b} < 0.45$ (BIN 2), $0.55 < \hat{b} < 0.65$ (BIN 3), and $0.75 < \hat{b} < 0.85$ (BIN 4), where $\hat{b} = b/b_{max}$. Here N/Z is changed by keeping the mass fixed. We use anisotropic standard isospin- and energy-dependent nn cross section $\sigma = 0.8 \sigma_{NN}^{free}$. The details about the elastic and inelastic cross sections for proton-proton and proton-neutron collisions can be found in Ref. [13]. The cross sections for neutron-neutron collisions are assumed to be equal to the proton-proton cross sections. It is worth mentioning that the results with the above choice of equation of state and cross section were in good agreement with the data [12, 14]. The reactions are followed until the transverse flow saturates. The saturation time varies from 100 fm/c for lighter masses to 300 fm/c for heavier masses. For transverse flow, we use the quantity "directed transverse momentum $\langle p_x^{dir} \rangle$ " which is defined as [15, 16]

$$\langle p_x^{dir} \rangle = \frac{1}{A} \sum_{i=1}^A \text{sign}\{y(i)\} p_x(i), \quad (5)$$

where $y(i)$ is the rapidity and $p_x(i)$ is the momentum of i^{th} particle. The rapidity is defined as

$$Y(i) = \frac{1}{2} \ln \frac{\mathbf{E}(i) + \mathbf{p}_z(i)}{\mathbf{E}(i) - \mathbf{p}_z(i)}, \quad (6)$$

where $\mathbf{E}(i)$ and $\mathbf{p}_z(i)$ are, respectively, the energy and longitudinal momentum of i^{th} particle. In this definition, all the rapidity bins are taken into account. A straight line interpolation is used to calculate E_{bal} .

Figure 1 displays the mass dependence of E_{bal} for four impact parameter bins. The solid (open) green circles

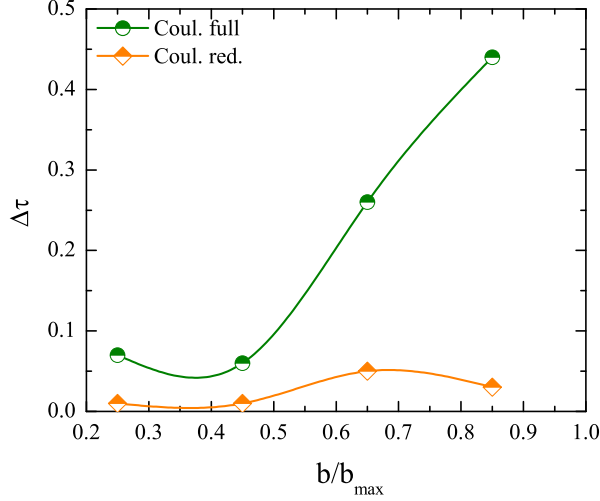


FIG. 2: τ as a function of reduced impact parameter. Lines are only to guide the eye.

indicate E_{bal} for systems with lower (higher) N/Z . Lines are power law fit $\propto A^\tau$. E_{bal} follows a power law behavior $\propto A^\tau$ for both $N/Z = 1$ and 1.4 (τ being labeled as $\tau_{1.0}$ and $\tau_{1.4}$ for systems having $N/Z = 1$ and 1.4 , respectively) at all colliding geometries. Also, for clarity we have not included very light system ($A=48$) as isospin effects are negligible at all colliding geometries for this system. From figure we see that isospin effects are clearly visible for all the four bins as neutron-rich system has higher E_{bal} throughout the mass range in agreement with the previous studies [9, 10, 12]. The magnitude of isospin effects increases with increase in mass of the system at all colliding geometries. The effect is much more pronounced at larger colliding geometries. One can see that the difference between $\tau_{1.0}$ and $\tau_{1.4}$ increases with increase in the impact parameter. In Ref. [14], Gautam and Sood studied the isospin effects on the mass dependence of E_{bal} for BIN 2. There they reduced the Coulomb potential by a factor of 100 and showed that the Coulomb repulsion plays dominant role over symmetry energy in isospin effects on E_{bal} as well as its mass dependence at semi central colliding geometry (BIN 2). Since here we plan to extend that study over a full range of colliding geometry, so here also we reduce the Coulomb potential by a factor of 100 and calculate the E_{bal} throughout the mass range at all colliding geometries. Solid (open) diamonds represent E_{bal} calculated with reduced Coulomb for systems with lower (higher) neutron content. Lines are power law fit $\propto A^\tau$. The values of $\tau_{1.0}$ ($\tau_{1.4}$) are -0.17 ± 0.02 (-0.14 ± 0.01), -0.17 ± 0.02 (-0.19 ± 0.02), -0.24 ± 0.03 (-0.26 ± 0.01), and -0.31 ± 0.03 (-0.29 ± 0.02) for BIN 1, BIN 2, BIN 3, and BIN 4, respectively. Interestingly, we find that the magnitude of isospin effects (difference in E_{bal} for a given pair) is now nearly same

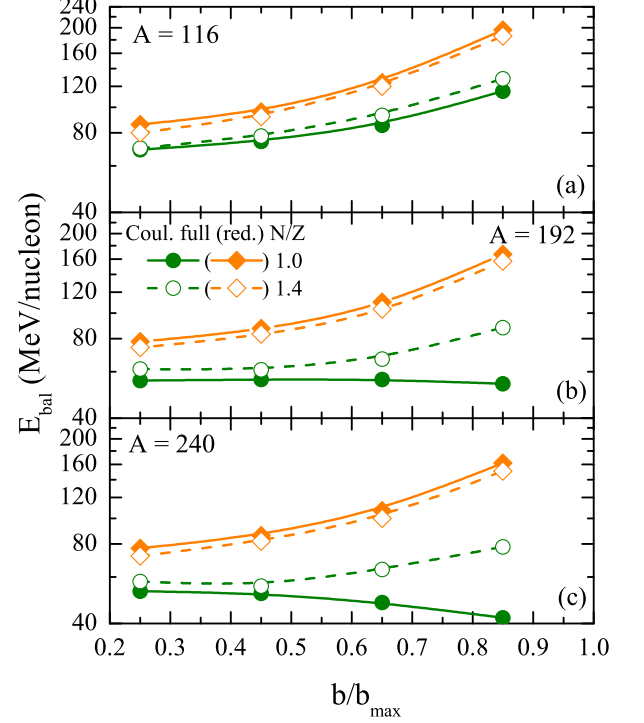


FIG. 3: E_{bal} as a function of impact parameter for different system masses. Symbols have same meaning as in Fig.1. Lines are only to guide the eye.

throughout the mass range which indicates that the effect of symmetry energy is uniform throughout the mass range. This is true for all the colliding geometries. This is supported by Ref. [17] where Sood and Puri studied the average density as a function of mass of the system (throughout the periodic table) at incident energies equal to E_{bal} for each given mass. There they found that although both E_{bal} and average density follows a power law behavior $\propto A^\tau$, E_{bal} decreases much sharply with the combined mass of the system (with $\tau = -0.42$), whereas the average density (calculated at incident energy equal to E_{bal}) is almost independent of the mass of the system with $\tau = -0.05$. It is worth mentioning here that the trend will be different at fixed incident energy in which case density increases with increase in the mass of the system [18, 19]. From fig. one can also see that the enhancement in E_{bal} (by reducing Coulomb) is more in heavier systems as compared to lighter systems for all colliding geometries. The effect is more pronounced at higher colliding geometries. Moreover, throughout the mass range at all colliding geometries, the neutron-rich systems have less E_{bal} as compared to neutron-deficient systems when we reduce the Coulomb. This trend is quite the opposite to the one which we have when we have full Coulomb. This (as explained in Ref. [14] also) is due to the fact that the reduced Coulomb repulsion leads to higher E_{bal} .

As a result, the density achieved during the course of the reaction will be more due to which the impact of the repulsive symmetry energy will be more in neutron-rich systems, which in turn leads to less E_{bal} for neutron-rich systems.

In fig. 2, we show the variation in $\Delta\tau$ as a function of colliding geometry for both full and reduced Coulomb where $\Delta\tau = \tau_{1.4} - \tau_{1.0}$. Half filled circles (diamonds) represent calculations with full (reduced) Coulomb. $\Delta\tau$ values are plotted at upper limit of impact parameter for each bin. Lines are only to guide the eye. From figure (green circles), we see that the difference between $\tau_{1.4}$ and $\tau_{1.0}$ increases with increase in impact parameter which is due to the sharp increase in value of $|\tau_1|$, whereas when we reduce the Coulomb (orange diamonds), this difference is negligible, which shows an enhanced effect of Coulomb at higher impact parameters.

In fig. 3a, 3b, and 3c, we display E_{bal} as a function of \hat{b} for masses 116, 192, and 240, respectively, for both full and reduced Coulomb. Symbols have the same meaning as in fig. 1. For full Coulomb (green circles), for all the masses at all colliding geometries, system with higher N/Z has larger E_{bal} in agreement with previous studies [9, 10, 20]. Moreover, the difference between E_{bal} for a given mass pair, increases with increase in colliding geometry. This is more clearly visible in heavier masses. Also for N/Z = 1.4, E_{bal} increases with increase in impact parameter as expected [20, 21]. However for N/Z = 1, this is true only for lighter mass system such as A = 116. For heavier masses E_{bal} infact begins to decrease with increase in impact parameter in contrast to the previous studies [9, 10, 12, 20, 21]. However, when we reduce the

Coulomb (by a factor of 100 (diamonds)), we find that:

(i) Neutron-rich systems have smaller E_{bal} as compared to neutron-deficient systems as mentioned previously also. This is true at all the colliding geometries throughout the mass range. This clearly shows the dominance of Coulomb repulsion over symmetry energy in isospin effects throughout the mass range at all colliding geometries.

(ii) The difference between E_{bal} for systems with different N/Z remains almost constant as a function of colliding geometry which indicates that the effect of symmetry energy is uniform throughout the range of \hat{b} as well. This also shows that the large differences in E_{bal} values for a given isobaric pair are due to the Coulomb repulsions.

IV. SUMMARY

We have studied the isospin effects in the disappearance of flow as well as its mass dependence throughout the mass range 48-270 for two sets of isobaric systems with N/Z = 1 and 1.4 in the whole range of colliding geometry. Our results clearly demonstrate the dominance of Coulomb repulsion in isospin effects on E_{bal} as well as its mass dependence throughout the range of colliding geometry. The above study also shows that the effect of symmetry energy on E_{bal} is uniform throughout the mass range and colliding geometry.

This work has been supported by a grant from Indo-French Centre For The Promotion Of Advanced Research (IFCPAR) under project no. 4104-1.

-
- [1] W. Zhan *et al.*, Int. J. Mod. Phys. E **15**, 1941 (2006); see, e.g. <http://www.impcas.ac.cn/zhuye/en/htm/247.htm>.
 - [2] See, e.g., http://www.gsi.de/fair/index_e.html.
 - [3] Y. Yano, Nucl. Inst. Methods B **261**, 1009 (2007).
 - [4] See, e.g., <http://ganiinfo.in2p3.fr.research/developments/spiral2>.
 - [5] See, e.g., White Papers of the 2007 NSAC Long Range Plan town Meeting, Jan. 2007, Chiacgo, <http://dnp.aps.org>.
 - [6] W. Scheid, R. Ligensa, and W. Greiner, Phys. Rev. Lett. **21**, 1479 (1968).
 - [7] A. Bonasera and L. P. Csernai, Phys. Rev. Lett. **59**, 630 (1987).
 - [8] D. Krofcheck *et al.*, Phys. Rev. Lett. **63**, 2028 (1989).
 - [9] B. A. Li, Z. Ren, C. M. Ko, and S. J. Yennello., Phys. Rev. Lett. **76**, 4492 (1996).
 - [10] R. Pak *et al.*, Phys. Rev. Lett. **78**, 1022 (1997); *ibid.* **78**, 1026 (1997).
 - [11] F. Daffin and W. Bauer, arxiv: 9809.0241v1.
 - [12] S. Gautam, R. Chugh, A. D. Sood, R. K. Puri, C. Hartnack, and J. Aichelin, J. Phys. G: Nucl. Part. Phys. **37**, 085102 (2010).
 - [13] C. Hartnack, R. K. Puri, J. Aichelin, J. Konopka, S. A. Bass, H. Stöcker, and W. Greiner, Eur. Phys. J. A **1**, 151 (1998).
 - [14] S. Gautam and A. D. Sood, Phys. Rev. C **82**, 014604 (2010).
 - [15] A. D. Sood and R. K. Puri, Phys. Lett. **B594**, 260 (2004); *ibid*, Eur. Phys. J. A **30**, 571 (2006).
 - [16] E. Lehmann, A. Faessler, J. Zipprich, R. K. Puri, and S. W. Huang, Z. Phys. A **355**, 55 (1996).
 - [17] A. D. Sood and R. K. Puri, Phys. Rev. C **70**, 034611 (2004).
 - [18] B. Blättel *et al.*, Phys. Rev. C **43**, 2728 (1991).
 - [19] D. T. Khoa *et al.*, Nucl. Phys. **A542**, 671 (1992).
 - [20] D. J. Magestro, W. Bauer, and G. D. Westfall, Phys. Rev. C **62**, 041603(R) (2000).
 - [21] R. Chugh and R. K. Puri, Phys. Rev. C **82**, 014603 (2010).